

# Quantum metrology with cold atoms

A Thesis

submitted to

Indian Institute of Science Education and Research Pune  
in partial fulfillment of the requirements for the  
BS-MS Dual Degree Programme

by

Satvika Bandrupally



Indian Institute of Science Education and Research Pune  
Dr. Homi Bhabha Road,  
Pashan, Pune 411008, INDIA.

May, 2018

Supervisor: Dr. C. M. Chandrashekar

© Satvika Bandarupally 2018

All rights reserved

# Certificate

This is to certify that this dissertation entitled Quantum metrology with cold atoms towards the partial fulfilment of the BS-MS dual degree programme at the Indian Institute of Science Education and Research, Pune represents study/work carried out by Satvika Bandrupally at Indian Institute of Science Education and Research under the supervision of Dr. C. M. Chandrashekar, Professor, Physics group, during the academic year 2017-2018.



Dr. C. M. Chandrashekar

Committee:

Dr. C. M. Chandrashekar

Dr. T. S. Mahesh

# Declaration

I hereby declare that the matter embodied in the report entitled Quantum metrology with cold atoms , are the results of the work carried out by me at the Physics group, Institute of Mathematical Sciences, Chennai, under the supervision of Dr. C. M. Chandrashekar and the same has not been submitted elsewhere for any other degree.

  
Satvika Bandarupally

# Acknowledgments

I would like to express my heartfelt gratitude to Prof Chandrashekar CM for the timely motivation and encouragement throughout the thesis. His guidance helped me immensely in all the time of research and writing of this thesis.

Besides my advisor, I would like to thank Prof Mahesh T S for giving me an opportunity to pursue my interested field at the correct time of my undergraduate studies. This helped me get an idea of the fundamentals of the subject.

Also, I would thank my colleague Alfred Ajay Aureate for the sincere help in my master's thesis.

Lastly, a special mention to my parents and my brother for overall support during this time.

# Contents

Abstract	ix
1 Introduction	1
2 General Procedure of Measurements	5
3 Multi-parameter Quantum Metrology	9
4 Metrology using Interferometry	11
5 Metrology in noisy environment	27
6 Quantum Zeno Effect	31
7 Quantum metrology with cold atomic ensembles	35
8 Conclusion	53

# Abstract

As quantum metrology advanced, it has achieved better sensitivity scaling in estimation of various parameters of different quantum mechanical systems. Interferometry is the most suitable method to perform measurements and implement the parameter estimation theories. We obtain interesting results when we merge the field of ultra-cold matter and quantum metrology. Here, numerical simulations of using a two-mode Bose Einstein condensate for performing Ramsay interferometry is presented. It is observed to attain the sensitivity scaling better than Heisenberg limit.

# Chapter 1

## Introduction

The physics of information and computing has been an acknowledged field since several decades. Information is an entity which can be encoded/concealed in the state of a system whereas computation is supposedly performed on a physical device. This would sum up to the fact that information and computing is the study of elementary physical processes. Before the advent of quantum mechanics into the world of physics, the transmission, storage and the processing of information was predominantly done using classical 'bits'. Since the laws of nature vary widely from atomic scale to our everyday object scale, it became essential to introduce theory which would best describe the observed phenomenon at microscopic scales. This need allowed the gradual growth of quantum mechanics. Although, this ideology sounded bizarre in the beginning, it did answer some serious observations such as the photoelectric effect and black-body radiation.

In an attempt to generalize the classical information theory to the microscopic world, quantum mechanics played a predominant role which lead to the emergence of quantum information theory where the data processing occurs in a quantum bit or a 'qubit'. There was a wild growth in this field when Peter Shor proved that the large numbers could be factorized using a quantum computer. There are lot of subtopics which study the physical properties of the information. Few include quantum cryptography, quantum error correction, quantum metrology and measurements and many more. My initial focus in this thesis will be majorly on the chronology of how quantum metrology came into picture along with describing the general procedure of measurements and interferometry while the latter part would consist



of the theoretical simulations of using Bose Einstein condensates from a metrological point of view.

Metrology by definition is the science performing a measurement. The term metrology originates from the greek word 'metron' and 'logos' which signifies 'the study of measurement'. The result may or may not be ambiguous/uncertain, but the sole art of making a measurement is the fundamental aspect of quantum information science. In other words, metrology means the art of formulating new strategies which allows us to extract the precise estimate of the parameter which is supposed to be measured. Estimation methods can be classified into two theories, one is global and the other is local theory. The global method lets us know the parameter needed to some precision without any initial knowledge about it while local theory helps when there is information about the interval where the parameter lies. It further enhances the achieved precision/accuracy. In these estimation theories the statistical quantity which determines the accuracy of the measurement is the variance of the estimator. We know from probability theory that cramer rao inequality lower bounds the variance of an estimator with the inverse of fisher information (described later). This fisher information contains the amount of information about the parameter in terms of probability distribution function. This rule can also be applied when we have to estimate multiple parameters at the same time. Although there may arise a problem due to non-commutativity of quantum measurements. The estimators corresponding to the lower bound are considered to be the most efficient ones. In comparison to this estimator, one can compare the output of the performed measurement check how much of error has occurred.

Formerly, these estimation theories were applied on classical or semi-classical systems. For example mechanical systems or optical systems described by classical wave optics. Usually, a typical estimation theory consists of 3 steps, probe preparation, interaction and then the probe readout. The kind of probe states we use lets us know how much amount of information about the parameter is encoded in the probe and helps in determining the precision of the measurement. The statistical errors can be minimized by repeating the interactions between the probe and the system independently for different measurements. The best scaling achieved for classical systems is termed as standard quantum limit (SQL) where the error scales as  $N^{-\frac{1}{2}}$ . Here  $N$  corresponds to the size of the probe which can be number of particles or modes of energy.

Eventually, when the quantum many body system problems were solved, these estimation

theories were applied on quantum mechanical systems. When the quantum systems chosen follow non-classical correlations, the precision obtained is called Heisenberg limit. This scales as  $N^{-1}$ . This enhanced scaling implies a better precision estimation in comparison to the classical systems which is the main reason why quantum metrology was well accepted. The fundamental limit can be obtained because of these precise estimations and they play an important role in gravitational field sensing using laser interferometry, precise time measurements in atomic clocks. It is observed that this Heisenberg limit could be achieved only for noiseless quantum systems. Although quantum error correction is a technique used to increase the precision where the system under consideration is shielded from noise.

Fundamental tasks of quantum metrology come under parameter estimation theory. The main objective is to be able to choose the best measurement scheme and then extract maximum possible information from the data retrieved. Usually, the second part of the objective is classical in nature. The experimental results can be looked at as outcomes of a classical random variable. As mentioned above, the fisher information can be maximized in the quantum setting of the experiment and quantum fisher information can be obtained. This will be the quantum version of the cramer rao bound rule (Quantum Cramer Rao rule). It is recognized that when quantum effects such as entanglement and squeezing are used in the quantum systems, there is a notable precision enhancement which occurs with respect to any classical system.

# Chapter 2

## General Procedure of Measurements

As mentioned above, the most general way of performing a measurement consists of 3 steps. Firstly, the probe is prepared in the required state and it should be let to evolve in time. This evolution is directly or indirectly dependent on the parameter to be estimated. Information about this parameter is extracted when the final measurement of the probe is performed. We choose a suitable observable  $\hat{O}$  which is dependent on the parameter, and operate it on the final state. Then we will get the expectation value of  $\hat{O}$  as a function of the parameter. As per the error propagation formula:

$$\Delta\theta = \frac{\Delta\hat{O}}{|\partial\langle\hat{O}\rangle/\partial\theta|} \quad (2.1)$$

where  $\Delta\theta$  is the error in measurement.  $\Delta\hat{O}$  is the variance in the Observable which is dependent on  $\theta$  and the denominator corresponds to the change of expectation value of the observable with respect to the parameter  $\theta$ . The standard deviation is given by

$$\Delta\hat{O} = \sqrt{\langle\hat{O}^2\rangle - \langle\hat{O}\rangle^2} \quad (2.2)$$

We see that the standard deviation of the parameter is dependent on itself. It is also described by POVM (Positive operator valued measure). The Positive operators  $E_x$  are the POVM elements associated with the measurement, and the set of all the  $\{E_x\}$ 's is a POVM. This set can be discrete or continuous or both. In POVM, the measurement

outcome is arbitrary. We are interested in knowing the probabilities of different outcomes. Projective Measurements are an example of POVM and these projective measurements are the special cases of general measurement where the operators are Hermitian and orthogonal projectors. They are known to give mathematical convenience and extra insight into quantum measurements. This whole Quantum Parameter estimation protocol can be understood as quantum network acting on a set of quantum systems. The probability distribution function of the output is given by Born Rule:

$$p(x|\theta) = \text{Tr}[E_x\rho(\theta)] \quad (2.3)$$

where  $p(x|\theta)$  is the probability distribution function of the parameter  $\theta$ .

As mentioned above the fisher information is dependent on the probability distribution function and that the maximum information about the parameter can be extracted from it. It is written as

$$F(\theta) = \int dx p(x|\theta) \left( \frac{\partial \ln[p(x|\theta)]}{\partial \theta} \right)^2 \quad (2.4)$$

In words, we can say that fisher information is the change of the probability distribution function with respect to the parameter i.e, for a little change in parameter there must be a considerable change in the observable which we have assumed to be dependent on the parameter. We can relate it to the understanding that the quantum system should be highly sensitive to the minor changes in the parameter. High response can be linked to how fast the system traverses in the Hilbert space.

## 2.0.1 Quantum Cramer Rao Rule

This rule sets a lower bound to the variance of the estimators in terms of Fisher Information. If we find an estimator that achieves this bound, then we have found the Minimum Variance Unbiased Estimator which is considered as the most efficient one. Although it is not guaranteed that MVUE does exist. This rule states that

$$Var(\theta) = \frac{1}{-E\left(\frac{\partial \ln[p(x|\theta)]}{\partial \theta}\right)^2} \quad (2.5)$$

The fisher information is never a negative quantity and can be added for independent observations made. It is a function on conditional probability of getting the value  $x$  when the parameter has the value  $\theta$ . However this rule can be applied to measurements done on more than one parameter. When we have multi parameter estimation being done, there is a chance of not saturating the cramer rao bound because of non-commutativity of the quantum measurements. Few examples where multi parameter measurement is done is imaging of electric, magnetic or gravitational fields in 3 or more than 3 dimensions.

## 2.0.2 Quantum Fisher Information

The fundamental limits the precision can achieve can be known from this term. This term not only stores information about the estimated parameter, but also measures the sensitivity a quantum system can provide, for example for performing phase sensitive tasks in interferometry. It is an extension of Classical Fisher Information. Surely, when entangled systems are considered the information obtained is beyond that of classical limit. But this does not occur for all entangled quantum systems. This may be because of the interaction between the quantum system and its surroundings which would lead to noise in the system. The effect the entanglement can be observed in the interaction terms of the hamiltonian. The maximization of the quantum fisher information with respect to it the parameter under consideration is done in the Quantum Cramer Rao rule. This whole theoretical structure of optimizing the sensitivity has had major impact in detecting the gravitational wave at LIGO.

As I have mentioned before the linkage between quantum fisher information and sensitivity, it can be better understood using the terms Bures metric. This metric signifies the statistical distance between the initial density matrix and the final state's density matrix. Sudden changes in parameter can be reflected as infinitesimal change in the distance. The quantum fisher information symbolizes the speed at which the initial state transforms into an orthogonal state. It can be said that large fisher information implies high sensitivity of the system, high speeds of evolution and high multi-particle entanglement. One advantageous

aspect of quantum fisher information is that, we don't necessarily have to know the process of the measurement. The knowledge of the initial and final state of the probe is sufficient to deduce the fisher information. Quantum fisher information in terms of initial and final state is expressed as

$$F_Q(\theta) = 4[\langle \psi'(\theta) | \psi'(\theta) \rangle - |\langle \psi'(\theta) | \psi(\theta) \rangle|^2] \quad (2.6)$$

Fisher information in terms of probability distribution function of the out come is given by

$$F_Q(\theta) = \int dx p(x|\theta) \left( \frac{\partial \ln[p(x|\theta)]}{\partial \theta} \right)^2 \quad (2.7)$$

# Chapter 3

## Multi-parameter Quantum Metrology

In all the metrological experiments, we try to optimize the quantum fisher information of the parameter under consideration. This in principle is done by saturating the quantum Cramer Rao bound. This bound can always be saturated if we are estimating a single parameter in the proposed experiment. There happen to be cases where one has to estimate the value of multiple variables. We try to get the best values of all the needed parameters with minimal uncertainties and errors. But the challenge arises when all these parameters have to saturate the quantum Cramer Rao bound simultaneously. This may not happen in all the cases because the quantum measurements corresponding to every parameter may or may not commute with each other. When this non-commutivity exists, one cannot saturate the quantum Cramer Rao bound. This aspect of quantum metrology is of interest because, it is observed that one obtains better precision results when these parameters are estimated simultaneously rather than the individual estimation of parameters. Also the fact that high precision multi-parameter quantum metrology has wide applications in fields like detection of gravitational waves, non-commutative geometry, imaging of fields, spectroscopy, quantum technology etc is responsible for the development in this field.

For a successful estimation of multiple parameters there should exist a state of the quantum system which would give the maximum sensitivity of all the parameters and a particular method which would be responsible for the non-commutativity of the individual parametric measurements i.e need for independent parameters. When these needs of the quantum system and their parameters are met, one would obtain a precision equivalent or perhaps

greater than the precision obtained by individual parameter estimation process. There were multiple estimation processes done using parameters such as one unitary parameter and the other noise parameter, say decoherence or estimation difference noise parameters in the same quantum system itself. This would be an efficient way of minimizing the noise in the system. Usually when we are focusing on one single parameter, we tend to build up the estimation process from the perspective of this parameter. This may lead to blowing up of the uncertainty of the other parameters under consideration. I find this mutual effect of having control on the parameters uncertainties analogous to Heisenberg uncertainty principle where greater precision in position would signify greater uncertainty in momentum. We can also relate it to spin squeezing in any of the two components. Therefore to avoid this unnecessary shooting up of uncertainty which is completely against the fundamental motive, we give specific weights to different parameters of interest and then devise a protocol based on this assumption.



# Chapter 4

## Metrology using Interferometry

Interferometry is the most appropriate method used for performing measurements. It uses the phenomenon of interference of waves with same frequency. The ones in phase interfere constructively and the ones out of phase interfere destructively. Small changes in the differences in the optical path can be detected when two waves are made to interfere. In order to generate an interference pattern of high precision, with distinctive fringes, we need a stable wavelength source: Laser. Typically, an interferometric procedure has an input beam which splits into two separate beams after hitting a beam splitter. These beams attain phase change while they are exposed to external environment and recombine using another beam splitter. The fringe pattern obtained can be used to make a measurement. This superimposition of beams to generate an interference pattern is the common principle used in any kind of interferometer.

As per theoretical and experimental observations, different initial states gave various metrological bounds for the parameters under measurements. Quantum entangled/squeezed states gave the Heisenberg limit whereas the classical states mostly reached the standard quantum limit. In interferometric experiments using optical states, the parameter estimated is usually the phase difference in the fringes. Mach-Zehnder interferometer is commonly used for phase measurements. While using cold atomic ensembles, parameter under estimation is coupling constant, phase shift between the modes and few other parameters (for Bose Einstein condensates). For interferometry with atomic matter, Ramsay interferometer is broadly used.

Interferometry using quantum states can be classified into single particle and multi particle states. With single particle states, this kind of measurement can give us insight into the degrees of freedom of the single particle used by comparing it to a simultaneous evolution of an ancillary system. Multi particle states are the systems where we can introduce quantum phenomenon such as entanglement or squeezing. This is how we know that the Heisenberg limit is the new limit set on metrological terms and we now need to know if there are any more effective systems which can result in a better precision oriented results. Theoretical claims say that this limit is broken by using 'two mode Bose Einstein condensate' in Ramsay interferometry. The second part of this thesis consists of how the Heisenberg limit is broken and better error scaling is obtained.

### 4.0.1 Single Particle States

For the sake of elaborate understanding of interferometry using single particle states, I describe how the relative phase difference follows the standard quantum limit in two different set ups. One is Mach-Zehnder interferometer and other is Ramsay interferometer.

#### **Mach-Zehnder Interferometry**

This interferometer was devised about a hundred years back and is still very commonly used for optical experiments and is named after Ludwig Mach and Ludwig Zehnder. It was devised in order to examine the wave-particle dual nature. This setup demonstrates interferometry by a simple mechanism. Because of the diffraction of the light waves, there is an interference pattern seen on the detector. The initial light beam is split into two modes by a beam splitter and then is recombined by a second beam splitter after certain interaction with external surroundings. During this exposure, two modes have had passed through different spatial paths and have attained phase difference. These two modes recombine either constructively or destructively at the detector/screen. From the resultant interference pattern, we can get the phase difference between the two modes. The reflection and partial transmission of the light waves at the beam splitters is responsible for change in phase. The phase shift dynamics are modelled by Fresnel equations in terms of how the wave behaves when it experiences spatial change in refractive index.

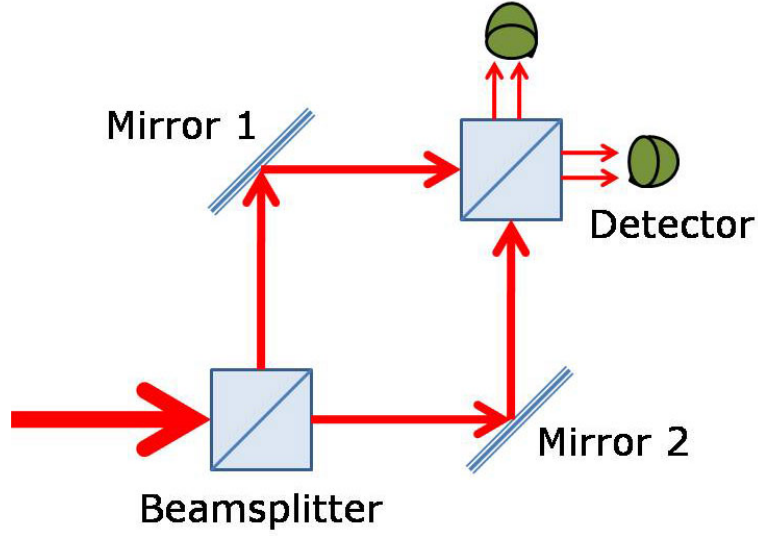


Figure 4.1: Mach-Zehnder Interferometer

Conventional schematic diagram of a Mach-Zehnder interferometer is given above.

Say, initially the state of the incident atom is  $|a\rangle$ . When it passes through the first beam splitter  $|a\rangle$  is split into a linear combination of two modes which can be written as

$$|\Psi_{in}\rangle = \frac{1}{\sqrt{2}}(|a\rangle + |b\rangle) \quad (4.1)$$

As mentioned above, the effect of the reflections and transmissions at the beam splitters can be expressed mathematically. Hence, the transformation matrix associated with the beam splitter is given by:

$$\hat{T} = \frac{1}{\sqrt{2}} \begin{bmatrix} 1 & 1 \\ 1 & -1 \end{bmatrix} \quad (4.2)$$

This transformation matrix acts on  $\Psi_{in}$ . After the accumulation of relative phase due to the external surroundings the state becomes

$$\Psi_{out} = \frac{1}{\sqrt{2}}(|a\rangle + \exp(i\varphi) |b\rangle) \quad (4.3)$$

where  $\varphi$  is the relative phase difference. The two modes merge subsequently and the state is converted into a final state given by

$$|\Psi_{out}\rangle = \hat{T}\Psi_{out} = \frac{1}{\sqrt{2}}[(1 + \exp i\varphi) |a\rangle + (1 - \exp i\varphi) |b\rangle] \quad (4.4)$$

The above state implies that the atom being in  $|a\rangle$  or  $|b\rangle$  mode is probabilistic in nature. The probability of it being in either state is given by

$$p(a|\varphi) = \cos^2(\varphi/2) \quad (4.5)$$

$$p(b|\varphi) = \sin^2(\varphi/2) \quad (4.6)$$

As we know the conditional probability of the outcome in terms of quantum fisher information (2.7). It can be applied here and is expressed as

$$\begin{aligned} F(\varphi) &= \frac{1}{p(a|\varphi)} \left[ \frac{\partial p(a|\varphi)}{\partial \varphi} \right]^2 + \frac{1}{p(b|\varphi)} \left[ \frac{\partial p(b|\varphi)}{\partial \varphi} \right]^2, \\ &= \sin^2(\varphi) + \cos^2(\varphi) = 1 \end{aligned} \quad (4.7)$$

Using Cramer Rao inequality, we can deduce the variance of the relative phase difference since we know the quantum fisher information. If this measurement is performed  $N$  times, the minimum uncertainty achieved is the standard quantum limit which is given by

$$\delta\varphi = \frac{1}{\sqrt{NF(\varphi)}} = \frac{1}{\sqrt{N}} \quad (4.8)$$

## Ramsey Interferometry

This interferometry was developed in order to study internal properties of an atom like the transition frequencies. The basic difference between Ramsey and Mach Zehnder interferom-

entry is that here the two beam splitters are replaced by  $\pi/2$  pulses. These beam splitters are spatially or temporally separated which when acts on the atom, helps in acquiring of relative phase between the energy levels. We can control the time difference as to when the  $\pi/2$  pulses are applied on the atom and it would reflect in the fringe pattern obtained. It is observed that if this time separation is maximum, highest sensitivity measurement is obtained. This technique is majorly used in atomic clocks where RF field is stabilized to obtain high precision measurement. To get a better visual of how beam splitters act on the two level atom, it is comfortable to view in a Bloch sphere. The first  $\pi/2$  pulse would act on the atom prepared in ground state, rotates it by  $\pi/2$  angle about the y-axis. The free evolution before the second pulse, would correspond to rotation by an  $\varpi$  around z-axis. Final pulse would rotate it by  $\pi/2$  around y-axis. The angle between the final state we have arrived at and z-axis is  $\varpi$ . If the atom is coupled to the external field, we can compare the atomic transition frequency to the frequency of the field. Here the Ramsey fringes are formed when the atom oscillates between the excited and ground state with respect to the time difference of when the first and second pulse is applied. Although the initial state is prepared in ground state, energies chosen for the ground and excited state is given by  $-w/2$  and  $+w/2$ . When the first pulse is applied the state becomes

$$|\varphi_{in}\rangle = \frac{1}{\sqrt{2}}(|\downarrow\rangle + |\uparrow\rangle) \quad (4.9)$$

where  $|\downarrow\rangle$  is the ground state and  $|\uparrow\rangle$  is the excited state. Then comes the free evolution of the states, hence the accumulation of the relative phase, which makes the state

$$|\psi_{out}\rangle = \frac{1}{\sqrt{2}}(e^{-i\varphi/2} |\downarrow\rangle + e^{+i\varphi/2} |\uparrow\rangle) \quad (4.10)$$

where  $\varphi$  is the phase difference. The procedure to get the standard quantum limit bound is similar to that of Mach-Zehnder interferometry. We get the probability distribution of whether the atom is in the ground state or excited state similar to the above case (4.6). Therefore the fisher information can be written as

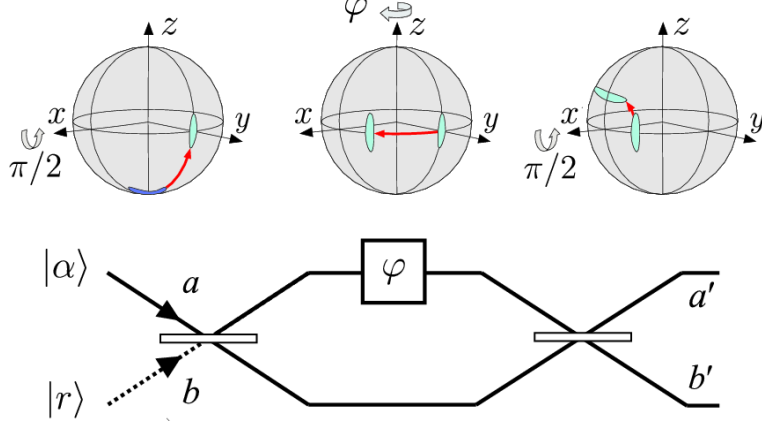


Figure 4.2: Bloch Representation of the process

$$\begin{aligned}
 F(\varphi) &= \frac{1}{p(\downarrow|\varphi)} \left[ \frac{\partial p(\downarrow|\varphi)}{\partial \varphi} \right]^2 + \frac{1}{p(\uparrow|\varphi)} \left[ \frac{\partial p(\uparrow|\varphi)}{\partial \varphi} \right]^2, \\
 &= \sin^2(\varphi) + \cos^2(\varphi) = 1
 \end{aligned} \tag{4.11}$$

Hence the uncertainty from quantum Cramer Rao inequality in the relative phase is given by

$$\delta\varphi = \frac{1}{\sqrt{NF(\varphi)}} = \frac{1}{\sqrt{N}} \tag{4.12}$$

We see that Ramsey interferometry performed with two level atom for phase estimation between the two energy levels attains the standard quantum limit too. This whole process can be represented diagrammatically by using a Bloch sphere (described above) as we know that points on the Bloch sphere represent the pure state of any 2 level quantum system. A simple figure showing this process is given above.

We consider the initial state as a vector pointing to the south pole of the sphere as shown in the diagram. In this case, there are two  $\pi/2$  pulses which represent the action of beam splitters. The first one corresponds to the rotation of the initial state by  $\pi/2$  degrees about y axis and then comes the free evolution which is nothing but the rotation of the state about z axis by an angle  $\phi$  which is the phase difference accumulated. And the final come the final

$\pi/2$  pulse which rotates the then state by an angle  $\pi/2$  around z axis.

## 4.0.2 Multi Particle states

There are lot of multi particle states which are useful to implement quantum interferometry. Since we have the control of introducing few quantum phenomenon like entanglement and squeezing within the particles, it is interesting to see how far the limit of minimal retrieval of error can be pushed beyond standard quantum limit. I will be discussing four such states: coherent spin states, spin squeezed states, NOON states and twin fock states.

### Coherent Spin States

Coherent spin states can be referred to as the pure quantum states of an ensemble of Spin - 1/2 particles of size N. This as a whole can be treated as a single spin particle of length  $N/2$ . If all these spins are aligned parallel to each other, it is called ferro-magnetic coupling whereas anti-parallel alignment of spins is called anti ferro-magnetic coupling. If we assume that all these N spin- 1/2 are polarized into one single state, the general form of coherent state can be written as

$$|\theta, \varphi\rangle_{CSS} = \otimes_{l=1}^N [\sin(\theta/2)e^{-i\varphi/2} |\uparrow\rangle_l + \cos(\theta/2)e^{i\varphi/2} |\downarrow\rangle_l] \quad (4.13)$$

If we consider the initial state to be spin down state (  $|\downarrow\rangle$  ), the above general equation of the state can be obtained by performing unitary rotations on the initial state (  $\otimes_{l=1}^N |\downarrow\rangle_l$  ) by an angle  $\theta$  and  $\phi$ . This state can also be shown diagrammatically by using a bloch sphere whose radius will be given as  $N/2$ . The direction of the final point obtained on the Bloch sphere is called as mean spin direction (MSD).

Ramsay interferometry with coherent spin states is done using the similar sequence of  $\pi/2$  pulses which is followed for single particle states. Here we assume that all the N spin- 1/2 particles aren't correlated i.e the direction of spins of all the particles are independent of each other. So as the first  $\pi/2$  is applied to the initial state, it transforms to

$$|\Psi_{in}\rangle = \otimes_{l=1}^N \left[ \frac{1}{\sqrt{2}} (|\uparrow\rangle_l + |\downarrow\rangle_l) \right] \quad (4.14)$$

We see that the state is transformed into equal superposition of the two available states similar to that of a two level atom splitting into two modes in a single particle state. After the free evolution is completed each state acquires a phase of  $\phi/2$  with respect to each other, and the final state is given by

$$|\Psi_{out}\rangle = \otimes_{l=1}^N \left[ \frac{1}{\sqrt{2}} (e^{-i\frac{\phi}{2}} |\uparrow\rangle_l + e^{+i\frac{\phi}{2}} |\downarrow\rangle_l) \right] \quad (4.15)$$

This sequence of pulses can be represented as vector transformations and rotations on the bloch sphere. Hence, the complete transformation to the final state can be expressed as a unitary transformation  $\hat{U}$ , given by

$$\hat{U} = \exp(-i\pi/2\hat{J}_y) \exp(-i\varphi\hat{J}_z) \exp(-i\pi/2\hat{J}_y) \quad (4.16)$$

This  $\hat{U}$  acts on the initial state as

$$|\Psi_f\rangle = \hat{U} |\Psi_0\rangle \quad (4.17)$$

Here,  $\hat{J}_x$ ,  $\hat{J}_y$ ,  $\hat{J}_z$  are the three collective spin operators which obey the commutation relation.

$$[\hat{A}, \hat{B}] = \hat{A}\hat{B} - \hat{B}\hat{A} \quad (4.18)$$

where  $\hat{A}$  and  $\hat{B}$  takes  $\hat{J}_x$ ,  $\hat{J}_y$ ,  $\hat{J}_z$  in the same cyclic order.

According to the error propagation formula 2.1, we can obtain the standard deviation of the phase difference. For this, we just need to know the variance of the  $\hat{J}_z$  operator and the rate of change of expectation value of  $\hat{J}_z$  with respect to  $\phi$ , which can be written as follows



$$(\Delta \hat{J}_z)_f^2 = (\Delta \hat{J}_z)_o^2 \cos^2 \varphi + (\Delta \hat{J}_y)_o^2 \sin^2 \varphi - \sin \varphi \cos \varphi \langle \hat{J}_z \hat{J}_z + \hat{J}_y \hat{J}_z \rangle \quad (4.19)$$

The standard deviation of the final state is given by

$$(\Delta \hat{J}_z)_f = \frac{\sqrt{N}}{2} \sin \varphi \quad (4.20)$$

Therefore we obtain the standard deviation of the phase  $\varphi$  as

$$\Delta \varphi = \frac{(\Delta \hat{J}_z)_f}{|\partial \langle \hat{J}_z \rangle_f / \partial \varphi|} = \frac{1}{\sqrt{N}} \quad (4.21)$$

So we observe that Ramsey interferometry using uncorrelated coherent states as initial states also obeys the precision bound set by standard quantum limit.

## Spin Squeezed States

Spin squeezing was initially studied in order to visualize correlations between multiple spins and also to produce entanglement between them as it is easy to produce them experimentally. This concept is applied widely in Bose Einstein condensates where we cannot distinguish the particles at that scale, but can introduce different kinds of correlations among them. They can be observed by defining spin operators for the ensemble as a whole where all the particles as a single unit. We know that there exist two complementary terms which satisfy the bound set by the Heisenberg uncertainty principle. Just like we have position-momentum, energy-time, we have the experimental control over the uncertainty on spins in different directions of measurement. By squeezed states it means, the fluctuations are reduced in one coordinate at the expense of the other one. The state where there are reduced fluctuations or reduced uncertainty is termed as spin squeezed state. This spin squeezing can be attributed to quantum entanglement in the system. This would lead to increase in the measurement precision.

Before we see how Ramsay interferometry is performed using spin squeezed states, we need to define certain terms named squeezing parameters. Since it is challenging to distin-

guish each single particle and manipulate the state at those length scales, the below defined parameters had to be constructed to describe the behaviour of the ensemble as a whole. The first parameter  $\epsilon_H$  is defined as follows

$$\xi_H^2 = \frac{2(\Delta\hat{J}_\alpha)^2}{|\langle\hat{J}_\gamma\rangle|}, \alpha \neq \gamma \in (x, y, z) \quad (4.22)$$

The subscript H represents Heisenberg uncertainty relation.  $\alpha$  and  $\gamma$  are orthogonal unit vectors. When the above quantity is less than 1, the state is said to be a spin squeezed state. The second parameter, gives us the information about the least uncertainty in the direction perpendicular to mean spin direction. It is given by:

$$\xi_S^2 = \frac{\min(\Delta\hat{J}_{\vec{n}_\perp})^2}{j/2} = \frac{4 \min(\Delta\hat{J}_{\vec{n}_\perp})^2}{N} \quad (4.23)$$

where  $n_\perp$  represents the direction perpendicular to mean spin direction. The reference state for these spin squeezed states are nothing but the coherent spin states. For uncorrelated coherent spin states, this term is equal to one. The ratio of the phase fluctuations of any general state to the uncorrelated coherent spin state gives us the third squeezing parameter. It is written as

$$\xi_R^2 = \frac{\Delta\phi}{(\Delta\phi)_{CSS}} = \frac{N(\Delta\hat{J}_{\vec{n}_\perp})^2}{|\langle\hat{J}\rangle|^2} \quad (4.24)$$

Now, while performing Ramsay interferometry using these spin squeezed states, we usually get a better precision in comparison to coherent spin states. The initial state in terms of the above defined collective spin parameters reads as follows

$$\langle\hat{J}_y\rangle_0 = 0, \langle\hat{J}_z\rangle_0 = -\frac{N}{2}, (\Delta\hat{J}_y)_0 = \frac{\sqrt{N}}{2}\xi_R, \quad (4.25)$$

We observe that the squeezing is performed along y-axis. Now this state undergoes a certain transformation due to the application of two  $\pi/2$  pulses and the free evolution. Therefore the expectation value of  $J_z$  reads as

$$\langle \hat{J}_z \rangle_f = -\cos \varphi \langle \hat{J}_z \rangle_0 + \sin \varphi \langle \hat{J}_y \rangle_0 \quad (4.26)$$

Hence, the variance is

$$(\Delta \hat{J}_z)_f^2 = (\Delta \hat{J}_z)_o^2 \cos^2 \varphi + (\Delta \hat{J}_y)_o^2 \sin^2 \varphi - \sin \varphi \cos \varphi \langle \hat{J}_z \hat{J}_z + \hat{J}_y \hat{J}_z \rangle \quad (4.27)$$

Therefore from the error propagation formula, the standard deviation of  $\phi$  is expressed as

$$\Delta \varphi = \frac{(\Delta \hat{J}_z)_0}{|\partial \langle \hat{J}_z \rangle_f / \partial \varphi|} = \frac{\xi_R \sqrt{N}/2}{|\sin \varphi| N/2} = \frac{\xi_R}{|\sin \varphi| \sqrt{N}} \quad (4.28)$$

This expression attains its minimum value when  $\sin \phi$  is 1. Therefore Heisenberg limit is reached when  $\xi_R = 1/\sqrt{N}$

It is observed that quantum fisher information has a strong condition to have entanglement rather than these spin squeezing parameters. But spin squeezing has its own advantages, it's easy to experimentally measure it and the change in sensitivity of this state can be related to the rotations in SU(2) space. This makes it easy to detect any quantum chaos in the evolution of the parameter.

## NOON States

A NOON state is a many-body entangled state. It is the superposition of all the N particles in say mode A and zero particles in mode B and vice versa. This state is said to give the maximum information about the phase in an interferometer (this implies the best precision). This entangled state doesn't follow the bell's inequality for quantum correlations. During interferometry, the difference in the number of photons travelling in the different spatial paths and the phase follow the number phase uncertainty relation. So this uncertainty in number is maximized, by making sure that all the photons are in either one path or the other. So, this would lead to the least uncertainty or fluctuation in the phase.

The general form of this state can be written as :

$$|NOON\rangle = \frac{1}{\sqrt{2}}(|N\rangle_a |0\rangle_b + e^{i\theta} |0\rangle_a |N\rangle_b) \quad (4.29)$$

The  $\theta$  represents the phase. These states are closely related to the GHZ states (Greenberger-Horne-Zeilinger States). The general form of an N-particle GHZ state is given by

$$|GHZ\rangle = \frac{1}{\sqrt{2}} \left( \left| \frac{N}{2}, +\frac{N}{2} \right\rangle + e^{i\theta} \left| \frac{N}{2}, -\frac{N}{2} \right\rangle \right), \quad (4.30)$$

Consider Ramsay interferometry with these GHZ states. The initial state is written as

$$|\Psi\rangle_{in} = \frac{1}{\sqrt{2}} \left( \left| \frac{N}{2}, +\frac{N}{2} \right\rangle + \left| \frac{N}{2}, -\frac{N}{2} \right\rangle \right), \quad (4.31)$$

During the free evolution, all the particles in the up/down state get entangled. So they acquire the same shift. The equation corresponding to this transformation of the state is given by

$$|\Psi\rangle_{out} = \frac{1}{\sqrt{2}} \left( e^{-i\frac{N\phi}{2}} \left| \frac{N}{2}, +\frac{N}{2} \right\rangle + e^{+i\frac{N\phi}{2}} \left| \frac{N}{2}, -\frac{N}{2} \right\rangle \right), \quad (4.32)$$

We don't need to know the probability distribution function of the output state to obtain quantum fisher information. Knowledge of the final state and its derivative with respect to the phase parameter is also sufficient to obtain quantum fisher information which is given as

$$F_Q(\theta) = 4 \left[ \langle \psi'(\theta) | \psi'(\theta) \rangle - | \langle \psi'(\theta) | \psi(\theta) \rangle |^2 \right], \quad (4.33)$$

This equation is quite useful because we need not know about the procedure of the measurement performed but just the initial and final states of the system. So, by differentiating the final state with the phase  $\phi$ , we will have

$$\frac{d|\Psi\rangle_{out}}{d\phi} = -\frac{iN}{2\sqrt{2}} \left( e^{-i\frac{N\phi}{2}} \left| \frac{N}{2}, +\frac{N}{2} \right\rangle - e^{+i\frac{N\phi}{2}} \left| \frac{N}{2}, -\frac{N}{2} \right\rangle \right) \quad (4.34)$$

Substituting this in the expression of quantum fisher information (4.33) we get the information term to be

$$F_Q^N = 4[\langle \psi'(\varphi) | \psi'(\varphi) \rangle - |\langle \psi'(\varphi) | \psi(\varphi) \rangle|^2] = 4\left(\frac{N^2}{4} - 0\right) = N^2 \quad (4.35)$$

Therefore, the error scales as

$$\Delta\varphi \geq \frac{1}{F_Q} = \frac{1}{N}, \quad (4.36)$$

We see that the uncertainty in phase attains the Heisenberg limit. Although while performing the experiment one should be careful as this state is quite vulnerable to particle losses which would disturb the precision.

## Twin Fock States

Twin fock states are the two mode states where the number of particles in each mode is equal. The input state is given as

$$|TWIN\rangle = |N\rangle_a |N\rangle_b \quad (4.37)$$

Preparation of these states using non-linear devices experimentally are still under construction. Twin fock states and spin squeezed states are said to be partially entangled states. This input state does not really attain the Heisenberg limit exactly, but asymptotically tends to it. We will see how that happens. The first beam splitter operator is given as follows

$$\hat{U}_{BS1} = \exp\left[\frac{\pi}{4}(\hat{a}\hat{b} - \hat{b}\hat{a})\right] \quad (4.38)$$

$\hat{a}$  and  $\hat{b}$  are the annihilation operators for the particles in the two modes. This beam splitter operator acts on the the initial state (4.37) and it transforms the twin Fock state to

$$|\psi\rangle_{BS1} = \sum_{k=0}^N C_k^N |2k\rangle_a |2N - 2k\rangle_b \quad (4.39)$$

The coefficients,  $C_k^N$  take the form

$$C_k^N = \frac{1}{2^N} (-1)^{N-k} \left( \begin{bmatrix} 2k \\ k \end{bmatrix} \begin{bmatrix} 2N-2k \\ N-k \end{bmatrix} \right)^{1/2} \quad (4.40)$$

During the free evolution the two modes  $a$  and  $b$  acquire a phase difference and the state then reads as

$$|\psi(\varphi)\rangle = \sum_{k=0}^N \exp i\varphi(2N-2k) C_k^N |2k\rangle_a |2N-2k\rangle_b \quad (4.41)$$

where,  $\varphi$  is the phase to be estimated. The second beam splitter operator is given by

$$\hat{U}_{BS2} = \exp[-i\frac{\pi}{4}(\hat{a}\hat{b} + \hat{b}\hat{a})] \quad (4.42)$$

This operator acting on the state which contains the phase difference (4.41) gives us the final state  $\hat{U}_{BS2}|\psi(\varphi)\rangle$

The last step performed is the parity measurement which should be done on either of the two modes. It is seen that this step is sensitive to phase measurements. This also scales the accuracy of measurement and helps in achieving the Heisenberg limit. This kind of measurement is performed even in Bose Einstein condensates, but the two modes here are analogous to the two hyper-fine levels in the atomic BEC. This parity operation acts at the detector placed at either of the modes, say mode  $b$  which is given as

$$\hat{\Pi}_b = \exp(i\pi\hat{b}\hat{b}) \quad (4.43)$$

We know that there should be a hermitian operator explicitly depending on the parameter, which we should let it evolve in time. It is from this operator we get to know the uncertainty in the parameter. This is encoded in the error propagation formula (2.1). In this case the hermitian operator is the parity operator. Therefore from the error propagation formula we will have

$$\Delta\varphi = \frac{\Delta\hat{\Pi}_b}{|\partial\langle\hat{\Pi}_b\rangle/\partial\varphi|} \quad (4.44)$$

It can be noticed that when  $\varphi$  tends to zero, Heisenberg limit is achieved. This limit goes below the standard quantum limit for some particular values of  $\varphi$  and total number of particles. Not only through the error propagation formula, also using the dependence of quantum fisher information on the initial and final states, we can derive the uncertainty in phase. From the later method, get the quantum fisher information to be

$$F_Q = 2N(1 + N) \quad (4.45)$$

According to the quantum cramer rao bound, uncertainty scales with number of particles as follows

$$\Delta\varphi = \frac{1}{\sqrt{2N^2 + 2N}} \quad (4.46)$$

This is observed to be in agreement with the phase uncertainty obtained by performing parity measurements for certain values of phase difference ( $\varphi$ ) and total number of particles ( $N$ ).

# Chapter 5

## Metrology in noisy environment

In all the above mentioned experiments performed with  $N$  number of initial particles, it is very natural for statistical (stochastic) and systematical errors to creep in. This may heavily affect the precision limit achieved. To some extent the statistical errors can be minimized by performing the measurement repeatedly which helps in better error scaling. We have achieved Heisenberg limit for some particular initial states, but parameters like decoherence or particle loss can go unnoticed which would lead to declined precision. This would have a substantial effect on quantum fisher information.

There are two types of noise which would affect the precision measurement in different ways. First one is when there is uncorrelated noise in the system. This can easily spoil the Heisenberg limit and the limit would fall down to standard quantum limit. But it is observed that this happens only for a certain limit of the particle number ( $N$ ). Secondly, when there is correlated noise in the system, which means, the system can be entangled with an ancilla system which is seen to give higher quantum fisher information which in turn gives better measurement. This occurs because when the quantum system is entangled with an ancilla, it becomes difficult for noise to creep into this entangled system. This whole system tends to act as one combined system only when the entanglement is optimized. We get higher quantum fisher information because, once the quantum system is entangled with an ancilla, we are expanding the hilbert space where the measurement can be performed. Now this higher dimensional hilbert space gives us more information about the parameter to be estimated.



Usually, the parameter to be estimated is not measured directly, but instead we choose a hermitian operator which explicitly depends on the parameter and this operator undergoes a unitary evolution along with the state evolution with time. We know that any unitary evolution can be distorted when the system interacts with the surroundings. Since the noise and external interactions cannot be avoided, this becomes a non-unitary evolution of the operator and the system as a whole. Because of this one cannot even maintain the precision to be asymptotically equivalent to Heisenberg limit. This is where we can introduce entanglement into the system to avoid various kinds of noise like phase damping, decoherence, depolarization etc. Although there are ways where phase-estimation is optimized for a two level system where entanglement was not used to enhance the precision.

Decoherence is the error that comes in due to the interaction with the environment when the quantum system evolves. Due to this one can say that the quantum element of the systems gets disrupted i.e there can be loss of entanglement in the system. It can either be a prolonged loss or loss in a finite small time period. The time depends on the kind of environment the system is in. Although, in spite of the noise being present everywhere, there are well optimized methods which measure the parameter. For example, methods have been devised for estimation of multiple phases (multi-parameter quantum metrology).

As I have explained above how the Heisenberg limit is achieved for maximally path entangled states i.e the NOON states in performing Ramsay interferometry. We see here how the noise brings about the fluctuations in the phase estimated. The major source of noise here is particle loss, as it may be difficult to keep all the particles entangled in the presence of an interacting environment. This makes it unsuitable for performing a measurement. States termed as  $mm'$  are seen to provide better robust metrological performance in the presence of noise. These states are just the generalized versions of path entangled NOON states. It is observed that performing parity detection measurements on the particles which are subjected to quantum phase fluctuations is the best estimation procedure to get the phase in a noisy environment.

General form of these  $mm'$  states can be written as

$$|m :: m'\rangle_{a,b} = \frac{1}{\sqrt{2}}(|m, m'\rangle_{a,b} + |m', m\rangle_{a,b}) \quad (5.1)$$

Here,  $a$  and  $b$  represent the two paths of the interferometer and  $m, m'$  are the number of photons incident at the two modes. This number is to be made optimum given the dynamics of loss i.e when the number of photons lost in the process is known. When we perform Mach-Zehnder interferometry with these states, after the first beam splitter, there is a phase shifter which is placed in one of the modes (say  $b$ ). This change in phase would correspond to the number of photons lost in the mode  $b$ . The state corresponding to the evolution up till the phase shift is given by

$$|\psi_u\rangle = \frac{1}{\sqrt{2}}(e^{im'\phi} |m, m'\rangle + e^{im\phi} |m', m\rangle) \quad (5.2)$$

After passing through the second beam splitter, just before the detection is performed the state reads as follows

$$|\psi_u\rangle = \frac{1}{\sqrt{2}}(e^{im'(\phi+\Delta\phi)} |m, m'\rangle + e^{im(\phi+\Delta\phi)} |m', m\rangle) \quad (5.3)$$

If we observe, we see that the state obtained before detection is a mixed state. This is due to the induced phase fluctuations in the path of one of the beams. The phase precision of both the NOON states and  $mm'$  states is measured by choosing the observable to be the parity operator. The general form of a parity operator is  $\exp i\pi n$ . This allows us to differentiate between even and odd number of photons. This parity operator operators only near one mode of the detector and inside the interferometer the parity operator reads as

$$\hat{\Pi} = i^{(m+m')} \sum_{k=0}^M (-1)^k |k, n-k\rangle \langle n-k, k| \quad (5.4)$$

From the error propagation formula, we just need to know the variance and expectation value of this parity operator to get to the final result.

$$\Delta\phi = \frac{\Delta\hat{\Pi}}{|\partial\langle\hat{\Pi}\rangle/\partial\phi|} \quad (5.5)$$

The error in phase measurement for the  $mm'$  states looks like

$$\Delta\phi_{mm'} = \sqrt{\frac{1 - e^{-2(\Delta m)^2\tau L} \cos^2(\Delta m\phi)}{(\Delta m)^2 e^{-2(\Delta m)^2\tau L} \sin^2(\Delta m\phi)}} \quad (5.6)$$

For the NOON state, it takes the form

$$\Delta\phi_{NOON} = \sqrt{\frac{1 - e^{-2N^2\tau L} \cos^2(N\phi)}{N^2 e^{-2N^2\tau L} \sin^2(N\phi)}} \quad (5.7)$$

We see that even for zero de-phasing for the  $mm'$  states, the precision of the phase can never be equal to Heisenberg limit but can only tend to it. But for the case of NOON states, this limit achieves Heisenberg precision under no de-phasing conditions.

Apart from all of this there is a method which is designed to protect the quantum system from the noise around it's surroundings. It is called quantum error correction. This can be applied when the noise isn't either too strong or highly correlated. If that is so it would be difficult go differentiate the source of the signals. It may be from the evolving Hamiltonian or from the noise in the system. This method helps in preserving the coherence in the system. But apparently this method is proved to be successful in reaching the Heisenberg limit.

# Chapter 6

## Quantum Zeno Effect

This effect can be said to be one of the paradoxical concepts of quantum mechanics. It is also termed as Turing paradox because this first came into texts when Alan Turing, a British scientist performed a thought experiment. Approximately, 30 years later the laboratory experiments were performed confirming this paradox. Given a quantum system in a well defined initial state. Under its free evolution according to its own Hamiltonian, if the observer keeps on making a projective measurement of the system on to its initial state, one can constrain the time evolution of the system and arrest the quantum system to the initial state. The state where the measurement is repeatedly performed is said to be a meta-stable quantum state. It is to be noted that this can occur only within a certain time limit which is the characteristic time limit given by

$$\tau_{QZ} = \frac{2}{\sqrt{F_Q[Q, A]}} \quad (6.1)$$

To actually witness this effect one should perform these measurements at a frequency greater than  $1/\tau$ . We see that Zeno time is inversely related to quantum fisher information. We can know information about the entanglement properties by observing the quantum Zeno effect of the quantum system. Quantum Zeno effect was observed in two hyper-fine levels of beryllium atom in ground state. These ions are trapped using penning trap or laser-cooling where we can apply the Rf pulses as per convenience which is responsible for making a measurement. Rf pulses are seen to easily manipulate the energy levels. The number of

photons scattered by the atoms in different hyper-fine levels is different. In one level there is no scattering which would make it easy for us to differentiate between the two hyper-fine states. We see that active measurement of energy levels of an atom actually effect the atom unlike from what happens in the macroscopic world where making a measurement wouldn't make a difference on the system. This occurs only at a quantum mechanical scale. When there is a spontaneous emission occurring between the two hyper-fine levels, if we perform a measurement continuously, it is observed that the way spontaneous emission occurs gets affected. The decay process of this transition process gets decelerated. This happens because each time we confirm that the atom is in the excited state, we reset the state of the atom to the excited state which means our activity of performing a measurement is fiddling around with the time scales of spontaneous emission. So till we stop measuring the state of the atom, it doesn't really come down to its lower energy level. In contrast to this, it was observed that frequent measurements in-fact accelerated the spontaneous emission or the decay process. This was termed as anti-Zeno effect. The speed of the decay can be attributed to the number of energy levels the electron can possibly jump into. More number of energy levels implies more chances of spontaneous emission, hence greater speed of decay. On the vice versa, less energy levels implies that the emission occurs at relatively low intervals of time which can be straight forwardly related to low decay speeds. So, it is possible to observe both Zeno effect and anti-Zeno effect experimentally by creating a microscopic circuit with its energy levels analogous to those of the atom's. The measurement of the state can be done by probing the circuit using microwave light at it.

Since we can make use of penning traps, we can trap multiple ions instead of probing a single ion with Rf pulses. Once there is an ensemble of ions in front of us, we will have to deal with effects of interactions between them. There can be interactions due to collisions when the observer probes the system with the Rf pulses. We can get to know the density matrix of the initial and final state of the ensemble and try to understand how the system has evolved irrespective of the repeated measurements being done. Also we can get a fair distribution of the ions in the two hyper-fine levels.

Also, when we are performing the measurement each time, we need to do it with a certain degree of accuracy so that the uncertainty of the measurement doesn't shoot up. The time required to make the measurement shouldn't affect the evolution time of the quantum system. It is seen that probability of this decay (above mentioned) in an atom is increases by four times, for short time intervals of repeated measurements. However to increase this time

interval, this atom can be coupled to a mode of a cavity by placing the atom in a resonant cavity. This coupling helps in increased oscillation of the atom between the two hyper-fine levels. The resultant dependence of probability of the spontaneous emission on the time intervals can be validated by actually demonstrating the experiment of atom coupled to a single mode cavity using a resonant cavity.

If we assume the existence of two eigen states  $X$  and  $Y$  for a quantum system under consideration. Say  $Y$  is the state where the system decays into. Whenever we perform a measurement, we know that the system collapses into  $X$ . In the time interval between the repeated measurements the system is said to exist in the superposition of the two states  $X$  and  $Y$ . To observe strong quantum Zeno effect, there should be finite time interval (frequency) between the measurements. Also the kind of system used to perform the measurement also has a major affect in observing this paradoxical effect.

As we have seen the significant developments of quantum metrology, it is very advantageous to know and understand it's applications in quantum optics and cold atomic physics. Since quantum mechanics has become the fundamental concept on which the technology works, like communication, information processing, cryptography etc, there is a need as to how the sensors in these technological devices work. This is a challenging task because in real life usage of these devices, the sensors are prone to lot of noise from the environment. So minimizing the error under these conditions is quite a useful task. This is where quantum metrology and it's precise measurements play a very major role. Major uses of quantum metrology are in quantum sensing, quantum RADARS, gravitational wave detection, quantum lithography etc. Interferometry is the significant tool to perform interferometry in the optical aspects. Apart from all of this, quantum metrology has a major applications in cold atomic matter and spectroscopy. The challenging part was to introduce entanglement between the atoms at such temperatures. Interesting results have been obtained by using cold atomic ensembles as the initial states of the interferometer. Phase estimation in atom interferometers and frequency estimation in atomic clocks is of great interest.

In the second part of this thesis, I would describe how Bose Einstein condensates can be used to perform Ramsey interferometry and how the Heisenberg limit of precision is broken in estimating the relative phase.

# Chapter 7

## Quantum metrology with cold atomic ensembles

### 7.0.1 Introduction

The cold atomic ensemble we consider here is the fifth state of matter i.e Bose Einstein condensate. In this state majority of the bosonic particles exist in their lowest quantum energy level at temperatures close to absolute zero. At this level of the temperature the quantum properties take over the classical ones. The condensate formed is observed to be a super-fluid i.e zero viscosity and also superconducting in nature. This state of matter was active in the theoretical context but wasn't actually prepared in the laboratory till the 1990's. This was partially due to lack of experimental setup which could reach the temperatures tending to absolute zero. The theoretical contribution was majorly done by Satyendranath Bose, an Indian physicist before he later contacted Albert Einstein for further ideas. Hence the name 'Bose-Einstein condensate'. At these low temperatures, the wave nature of the bosons become predominant, since all the particle are identical, all the particles in the ensemble will have similar wave functions. With the decrease in temperature, these wave functions begin to condense and hence overlap with each other. After the overlap, the state of the condensate is represented by a single wave function with the energy equal to that of ground state energy of the particle's. It is to be noted that the final state achieved isn't a solid state. If we have  $N$  identical bosons at a particular temperature  $T$  with the chemical potential  $\mu$ , the energy distribution of the condensate follows Bose Einstein statistics which

is given by

$$f(\epsilon) = \frac{1}{\exp(\epsilon - \mu)/k_B T - 1} \quad (7.1)$$

From this expression we see that as the temperature approaches to absolute zero, the lowest energy level is maximally occupied. This is when the whole ensemble of  $N$  bosons acts as a single particle. This is termed as quantum phase transition. This doesn't necessarily happen at absolute zero temperatures experimentally, but close to it would result in phase transition. The de-Broglie wavelength of the particles dependence on the temperature is given by

$$\lambda_{db} = \frac{h^2}{2\pi m k_B T} \quad (7.2)$$

where  $h$  is the planck's constant,  $m$  is the mass of the bosons and  $k_B$  is the Boltzmann constant.

We can confirm the formation of the condensate by observing the velocity distribution of the bosons. At normal temperatures, the bosons are comparatively widely distributed on a velocity space. As the temperature keeps on decreasing, we can observe a peak at lowest (mostly zero) velocity and the peak drastically falls off with increasing velocities.

This phase transition occurs only when the system drops down below a certain temperature. It is termed as critical temperature and is given by

$$T_c = 3.31 \frac{\hbar^2 n^{2/3}}{m k_B} \quad (7.3)$$

where  $n$  is the particle density,  $m$  is the mass per each boson and  $k_B$  is the Boltzmann constant.

We can know the fraction of atoms in the condensed state by the formula

$$f(T) = 1 - (T/T_c)^{3/2} \quad (7.4)$$



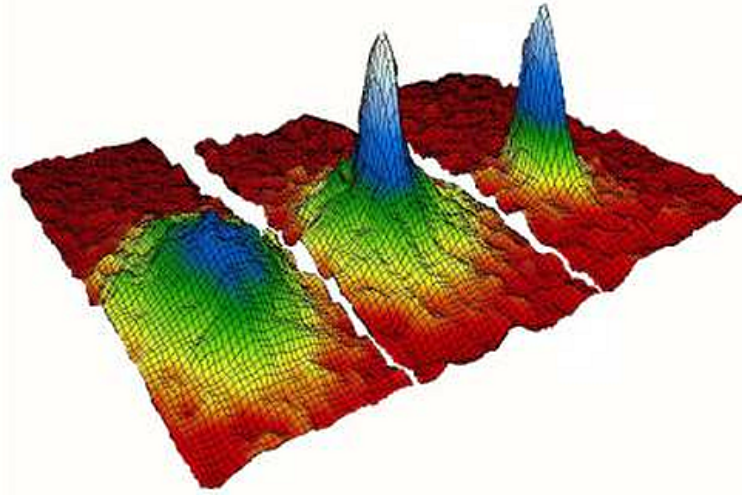


Figure 7.1: Velocity distribution at different temperatures

At this level there can be weak interactions in the condensate and we need to know how to quantify them in order to understand the dynamics of the new state of matter obtained. The effect of the interactions can be seen in the spatial spread of the wave function. Usually at high temperatures, the gas of atoms or the bosons have their total energy contributed by accessible degrees of freedom like rotational, translational and vibrational. They have different thresholds of temperature for them to make a significant contribution. As the temperature is dropped down to room temperatures, there is no vibrational energy as the vibrations of the atoms/bosons is frozen out. There will just be rotational and translational degrees of freedom. When the temperature is further lowered, we are left only with translational motion of the atoms. Quantization of this thermal energy occurs at low temperatures where the quantum effects become predominant. This is when the overlap of all the similar wave functions occur. There are chances that the gas may condense at these temperatures because of the interactions. There should be measures taken to prevent this condensation. So, ideally the gas should have zero interactions and in experiments minimal interactions among the atoms is appreciated.

Clearly, this kind of phase transition occurs only with bosonic particles. By bosons, I mean the spin of the whole atom (all the protons and electrons combined) should bear an integral value. Any other fractional value is considered to be a fermion. These fermions are subjected to Pauli exclusion principle which is responsible for interaction energy that makes it not possible to achieve the zero-velocity state.

We see that since the quantum nature of the bosons come into picture in the condensate, the wave function of each particle extends up to it's own wavelength. The dependence of this wavelength with respect to the temperature is given as

$$\lambda_{deB} = \frac{h}{\sqrt{3mk_B T}} \quad (7.5)$$

The explanation for the wave functions overlapping can be understood from this expression. As the temperature is lowered we can notice that wave function extends over a longer length, which is responsible for the interaction of the wave functions. The extended state of the whole interaction is the Bose Einstein condensate with a single wave function. These condensates weren't prepared till the 90's in laboratory. The first basic step is to cool down and trap the atoms using the laser cooling techniques and the second important step is to further cool these atoms using the technique of evaporative cooling which helps us reach temperatures to the order of micro kelvin.

Evaporative cooling technique is the most utilized technique and is immensely responsible for the development of experimental aspects of ultra cold matter. The first step in this process is to trap the atoms at the room temperature. Magnetic traps are used for this where the highest velocity or the highest energy atoms let themselves out of the trap thus collecting the lower energy atoms inside the trap. Small part of the temperature gets reduced here. To thermalize the elastic collisions between the atoms, the height of the magnetic potential walls are reduced. This accelerates the loss of higher energy particles. The counter effect of this is the remaining particles in the trap get condensed eventually.

If we look into this, when the atoms are placed in the magnetic field, the splitting of the energy levels occur due to the interaction between the dipole moment of the atom and the magnetic field. Basically, Zeeman splitting occurs. There are two kinds of splitting that occur in the magnetic field. The levels which whose energy rises in the presence of the magnetic field are called as low-field seekers and the vice versa occurs for high-field seeker energy levels. Depending of what kind of energy level atoms we want to trap, we can create minimas or maximas for the atoms to get trapped. But creating a magnetic potential maxima contradicts Earnshaw's theorem. Therefore for experimental purposes, local minimas are created in order to trap low-field seeking atoms.

The experimental success of creating a BEC has led to test different properties of a condensate and a theoretical interest since then. The dynamics of the behaviour of these Bose Einstein condensates in the magnetic trap potentials is described by Gross Pitaevskii equations. This description of atomic behaviour at such temperature scales makes a BEC more relevant in metrological aspects. Ramsay interferometry using a Bose Einstein condensate was performed and interesting results have been observed. The BEC used is said to be a two mode BEC. Before I go into the precision measurements of the coupling constant (estimated parameter) in the condensate, I would first explain what a two mode theory in a Bose Einstein condensate is.

We know that when the condensate is formed all the bosons occupy a single ground state which can be termed as a mode too. But while performing interferometric experiments, we need interference between condensates present in different modes or energy levels because we get the fringes due to the phase difference established. From the fringes obtained we can know the information about the spatial positions of the bosons. When the condensates in the two modes superpose, there obviously will exist interactions between the atoms. This may introduce some non-linear terms in the hamiltonian which would be responsible for noise in the fringes such as de-phasing. This disturbance in the interference patterns can be avoided if the BEC is made up of photons or magnons, where there isn't any kind of interaction. So, to achieve two modes in a single condensate double well magnetic potentials are used, where the lowest energy (ground state) mode is the condensed part of the system whereas the other well would contain the atoms in the next immediate hyper-fine energy level, which is the non-condensed part of the system. These two states co-exist and their evolution is studied by solving Gross Pitaevskii equations.

The first step in interferometry using a BEC is that the initial state is prepared in a ground state. All the  $N$  atoms are supposed to be in lowest energy state whose wave function is given by  $\phi_1(r)$ . After some time, the double well potential is turned on, which excite some of the atoms into the next hyper-fine level. This excited state is the anti-symmetric one and the ground state is the symmetric state. The symmetric breaking occurs when the double well is created. The particle's wave function in the excited energy level is given by  $\phi_2(r)$ . This initial state is created for not a large atom number, to avoid unnecessary interactions which would affect the fringe pattern obtained. Therefore small boson number is considered to be advantageous.

The BEC fragmenting into two modes can be analytically studied by comparing it with two harmonic oscillators separated by some finite distance and with a wall. These two oscillators with same frequency can be considered as the eigen states of both the symmetric and anti symmetric modes in a BEC. The potential felt by the condensed and non-condensed particles of the BEC is different. Hence the difference in potential in the Schrodinger equation would give us two different wave functions after certain period of evolution. BEC fragmenting into two modes allows us to consider the ensemble as a giant spin system of certain spin length.

There is a factor  $\eta_N$  which signifies the spread of the BEC wave function. It is the inverse of volume occupied by the ground state wave function which is written as

$$\eta_N = \int d^3r |\psi_N(\vec{r})|^4 \quad (7.6)$$

where  $\psi_N$  is the ground state condensate wave function which satisfies the below Schrodinger equation

$$\left( -\frac{\hbar^2}{2m} \nabla^2 + V(\vec{r}) + g_{11} N |\psi_N(\vec{r})|^2 \right) \psi_N(\vec{r}) = \mu_N \psi_N(\vec{r}) \quad (7.7)$$

$V(\vec{r})$  is the trapping potential used to trap the bosons. The potential has two components, one being transverse harmonic potential and other being power law potential. The general form of the potential can be expressed as

$$V(\rho, z) = \frac{1}{2} (m\omega_T^2 \rho^2 + kz^q) \quad (7.8)$$

Graphically, the potential varies with respect to  $z$  for different values of  $q$  as given below.

In the longitudinal dimensions, it is the power law potential that traps the atoms whereas in the transverse dimensions, it is the harmonic potential.  $q$  here is the significant parameter in the whole experiment. The value of  $q$  defines the hardness of the longitudinal trap. The hardest trap has infinite value of  $q$ . We can observe a significant change in the spread of the wave function i.e  $\eta_N$  with a slight change in  $q$ . The existence of hard walled potential helps to reduce the spread of the wave function in the longitudinal direction. This helps us to study

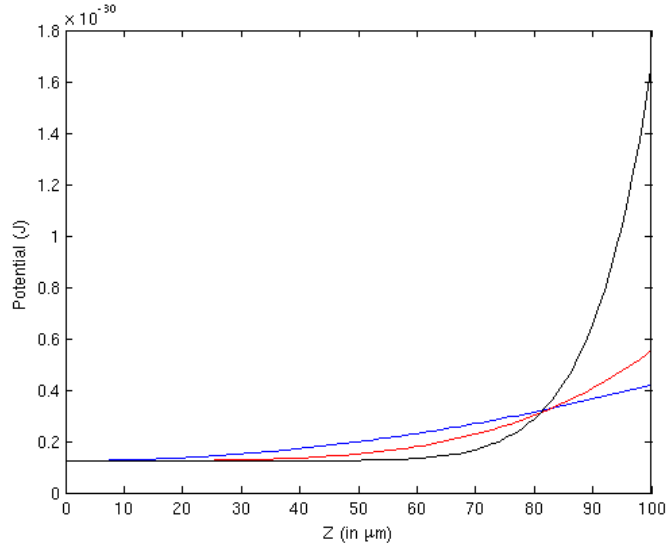


Figure 7.2: Potential with respect to  $z$

the dependence of number of atoms and the extent to which the wave function spreads. The  $\rho$  here implies that the harmonic potential exists in the transverse coordinates. Atoms here are trapped tightly in the transverse directions relative to the longitudinal direction. Hence the spreading of the BEC wave function in the transverse direction is neglected.

$g_{11}$  is the scattering coefficient which quantifies the intra species interaction in the BEC. This is dependent on the s-wave scattering length as follows

$$g_{11} = \frac{4\pi\hbar^2 a_{11}}{m} \quad (7.9)$$

$a_{11}$  is the s-wave scattering length which exists for interaction among condensed atoms, among non condensed atoms and between condensed and non-condensed atoms of the BEC and  $m$  is the atomic mass.

While performing interferometry with Bose Einstein condensates, there are two approximations considered. First one being Josephson approximation and the other being Thomas-Fermi approximation. Josephson approximation says that the two mode wave functions retain their wave functions. This is approximated for a certain time interval, because it is obvious that there will be interaction with the surroundings which would induce position dependence phase shifts. Thomas Fermi approximation neglects the particle's kinetic energy

at low temperatures. This is a great approximation for large number of particles and doesn't really work well for small number.

The Josephson approximation works aptly when we do not give time for the each mode wave functions to evolve. This can be done by allowing fast transitions between the two energy levels. Apart from this, we assume that the depletion of ground state wave function is small that it is neglected. Non-linear Ramsay interferometry performed with the rubidium BEC which is maintained in two hyper fine levels, apparently gives us the best scaling of the precision. In fact better than the Heisenberg limit (greater than  $1/N$ ). Although the sensitivity is affected by external interactions (via surroundings), this effect can be minimized by performing the metrological measurements at low time scales where significant interaction which would lead to decoherence and phase irregularities haven't crept into the system. Because of the Josephson approximation and the limit time scale window we have chosen to make a measurement, the phase induced is the differential phase shift but not position dependent phase shift.

The BEC used here for performing Ramsay interferometry is made up of rubidium-87 atoms which is confined to two hyper-fine levels. This condensate was first achieved in 1995 and approximately 170 nano kelvin of temperature was reached in preparing this. The techniques used were laser cooling and magnetic evaporative cooling. This atomic sample is observed to have negative scattering length.

## 7.0.2 Gross–Pitaevskii equations

After successfully achieving the condensates experimentally in laboratories, there was a push in the theoretical front to predict the dynamics of the atoms in a BEC. Under few assumptions and approximations, modelling of the ultra cold matter has been done which lead to Gross–Pitaevskii equations. Solving these equations gives us an accurate form of the wave function of the condensate present in two hyper-fine levels. These equations are modelled by mean field theory approximations which signify weak interactions at low temperatures.

Most of the solutions for these equations are solved within the Thomas-Fermi limit. In the Thomas-Fermi range, the kinetic energy of the atoms individually is relatively less in comparison to the interaction energy in the condensate. Therefore, the kinetic energy term

in the Schrodinger equation is neglected. Although the size of the condensate can be know by something called Thomas-Fermi limit which will be discusses later.

The nonlinear Schrodinger equation which describes the dynamics of a BEC trapped in some potential is written as

$$\mu_N \frac{\partial \psi}{\partial t} = \left( -\frac{\hbar^2}{2m} \nabla^2 + V_{ext} + gN|\psi|^2 \right) \psi \quad (7.10)$$

$V_{ext}$  is the trapping potential uses to confine the bosons.  $g$  is the scattering coefficient which is dependent on s-wave scattering length as  $g = \frac{4\pi\hbar^2 a_{11}}{m}$ , this is the interaction term.  $|\psi|^2$  is the atomic density and  $N$  is the total number of atoms in the ground state.

$\mu_N$  is the chemical potential of the condensate. Chemical potential is basically the increase in amount of energy of the condensate when one boson is added to the system. This value of energy allows us to know how strong the interactions are among the bosons. When one assumes zero interaction or if one can possibly switch of the interactions, the chemical potential is equivalent to the single particle energy. It is written in terms of free energy of the condensate as

$$\mu_N = \left( \frac{\partial F}{\partial N} \right)_{V,T} \quad (7.11)$$

The Hamiltonian of this two-mode Bose Einstein condensate can be expressed as

$$\hat{H} = NE_o + \frac{1}{2} \eta_N \sum_{\alpha,\beta=1}^2 g_{\alpha\beta} (\hat{a}_\beta)^T (\hat{a}_\alpha)^T \hat{a}_\alpha \hat{a}_\beta \quad (7.12)$$

$(\hat{a}^T)_\alpha$  creates the atoms in the condensate i.e annihilation of the atoms in the state  $|\alpha\rangle$

After inculcating the Josephson approximation in knowing the dynamics, the two mode hamiltonian of the system can be modified and written in terms of angular momentum operators. Assume the expression of  $\hat{J}_z$  to be (in terms of creation and annihilation operators)

$$\hat{J}_z = \frac{\hat{a}_1^t \hat{a}_1 - \hat{a}_2^t \hat{a}_2}{2} \quad (7.13)$$

The two coupling constants,  $\gamma_1$  and  $\gamma_2$  signify the strength of the interaction between the atoms are given as follows

$$\begin{aligned} \gamma_1 &= \frac{1}{2}(g_{11} - g_{22}) \\ \gamma_2 &= \frac{1}{2}(g_{11} + g_{22}) - g_{12} \end{aligned} \quad (7.14)$$

Now, the two mode hamiltonian can be modified for including Josephson approximation as follows

$$\hat{H} = \gamma_1 \eta_N N \hat{J}_z + \gamma_2 \eta_N \hat{J}_z^2 \quad (7.15)$$

The  $\hat{J}_z^2$  term is responsible for entanglement between the two modes and also the phase diffusion in the interference pattern where as the  $\hat{J}_z$  term signifies the differential phase shift induced in the beginning time interval where the surroundings don't play a significant role in interaction with the mode evolution.

We call this to be a non-linear Ramsay interferometry because this non-linearity in the hamiltonian arises from the interactions between atoms. Because of these interaction between the coherent atoms, interesting observations like nonlinear tunneling and new interference patterns emerge in the system. From the experimental results, it is confirmed that the frequency in the fringes obtained during a spread of time where the allowed approximations break down, gives us significant information about the strength of the non-linear interactions and the symmetry breaking between the two modes. The condensed, zero momentum state is supposed to be symmetric in nature and the non-condensed, finite momentum state is anti symmetric in nature. So, when we excite some of the ground state atoms into the next hyper-fine level, symmetry breaking occurs. This can be interpreted from the obtained nonlinear fringe pattern which significantly deviates from the linear type fringe pattern.



### 7.0.3 Spreading of a BEC wave function

The fundamental need of using the term  $\eta_N$  to describe the volume of the condensate. As mentioned previously, the effect of change in volume of wave function with respect to the number of atoms in the condensate is responsible for the sensitivity in the precision obtained. The change in volume is because of the change in energy levels of the atoms in the condensate which affects the kinetic energy of the condensate as a whole. This can be controlled by changing the hardness of the applied potential. We know that when there are less number of atoms in the condensate, there will be less repulsive interactions. The opposite case is slightly problematic because since with more number of atoms the repulsions are strong, the condensate tends to push itself into new dimensions. When this occurs, the effective interactions gets diminished as it is a function of the volume the condensate is present in. This would affect the scaling in the sensitivity measured.

The potential used to trap the atoms in the condensate is of the form

$$V(\rho, z) = \frac{1}{2}(m\omega_T^2\rho^2 + kz^q) \quad (7.16)$$

Greater the value of  $q$ , harder is the potential. With the increasing hardness in the potential, we can say that the expansion of the BEC ground state wave function can reduced. The transverse harmonic potential is higher than the power law potential in magnitude. Hence, we can say that atoms in  $\rho$  direction are tightly confined spatially rather than the ones in  $z$  direction.

We get the dependence of  $\eta_N$  on number of atoms ( $N$ ) and the hardness of the potential ( $q$ ) by integrating the following equation

$$\left( -\frac{\hbar^2}{2m}\nabla^2 + V(r) + g_{11}N(|\psi_N|)^2 \right)\psi_N(r) = \mu_N\psi_N(r) \quad (7.17)$$

This is a time independent, three dimensional Gross Pitaevskii equation which is integrated using GPE toolbox in MATLAB. In the process of solving this equation, the first approximation considered is

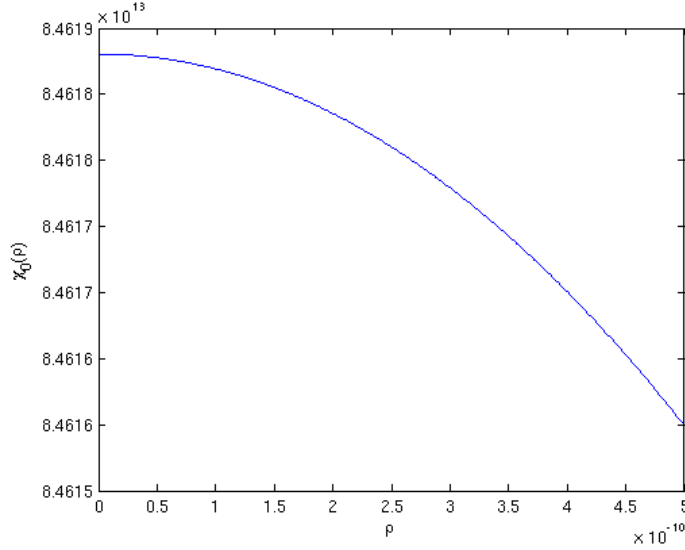


Figure 7.3: Ground state wave-function of transverse harmonic potential

$$\psi_N(\rho, z) = \chi_o(\rho)\phi_N(z) \quad (7.18)$$

$\chi_o$  is the ground state wave function of the transverse harmonic oscillator and  $\phi_N(z)$  is the solution of one dimensional Gross Pitaevskii equation

$$\left( -\frac{\hbar^2}{2m} \frac{\partial^2}{\partial z^2} + \frac{1}{2}kz^q + g_{11}N\eta_T(|\phi_N|^2) \right) \phi_N(r) = \mu_N \phi_N(r) \quad (7.19)$$

$g_{11}$  quantifies the scattering interactions in the condensate and  $\eta_T$  is the inverse of the transverse cross-section occupied by the condensate. It is given as

$$\begin{aligned} \eta_T &= \frac{1}{2\pi\rho_o^2} \\ \rho_o &= \sqrt{\frac{\hbar}{m\omega_T}} \end{aligned} \quad (7.20)$$

The graph of  $\chi_o(\rho)$  and  $\phi_N(z)$  is given above

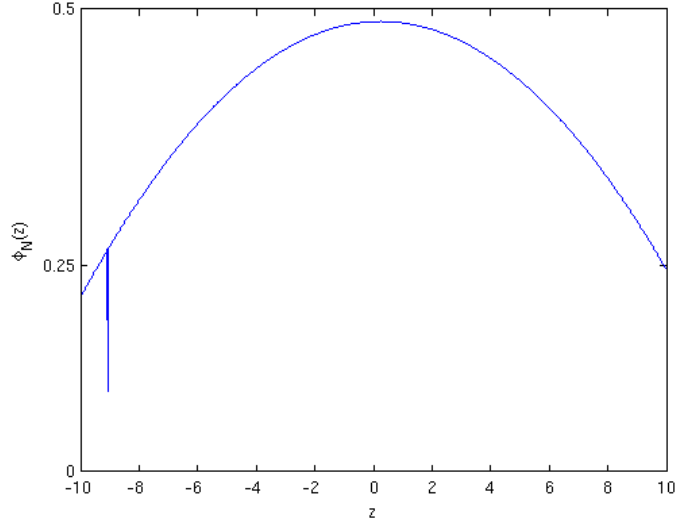


Figure 7.4: Ground state wave function for longitudinal potential

The relation between  $eta a_N$  and number of atoms in the condensate for different  $q$  is as follows

$$\eta_N = \frac{q}{2q+1} \left(\frac{q+1}{1}\right)^{\frac{q}{q+1}} \left(\frac{k}{Ng_{11}}\right)^{\frac{1}{q+1}} \left(\frac{1}{2\pi\rho_o^2}\right)^{\frac{q}{q+1}} \quad (7.21)$$

If we observe the plots, there is a sudden change in slope in at a certain value of  $N$ . This value of  $N$  is called critical atom number. At this or beyond this number of atoms in the condensate, the scattering interactions rise drastically, which would lead to increase in scattering energy greater than the transverse kinetic energy of the atoms. So, usually in the equation (7.19) , when number of atoms reached the critical atom number the kinetic energy terms can be neglected.

These results are compared with the solutions of the one dimensional and two dimensional Gross Pitaevskii equations, where Thomas Fermi approximation is considered. Below the critical atom limit, the condensate is restricted to transverse dimensions and it isn't allowed to spread in radial directions. The reason of the spread in radial direction beyond the critical atom limit is because at this level of scattering energy, the longitudinal potential isn't sufficient to confine the atoms spatially.

However the relation between  $\eta_N$  and number of atoms in the condensate for different

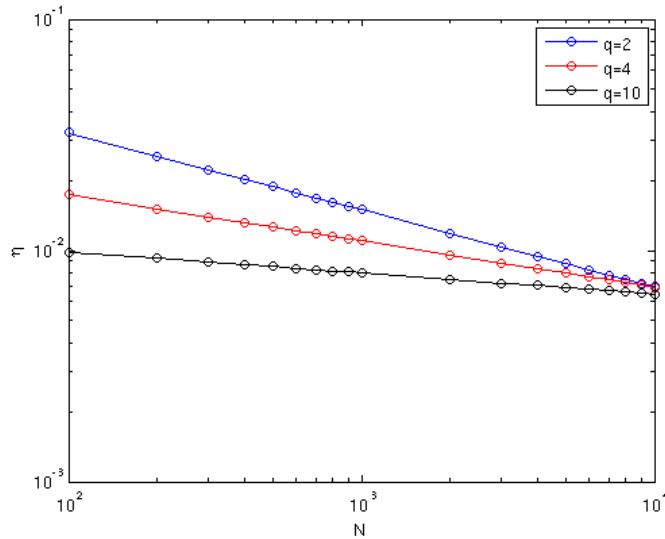


Figure 7.5: Change of  $\eta_N$  with  $N$  for different  $q$

$q$  is not the above linear relation. It varies as  $N^{-(q+1)/(2q+1)}$ . The dependence of  $\eta_N$  with respect to  $N$  for different values of  $q$  is given below

#### 7.0.4 Ramsay Fringes

We need to observe and analyze the Ramsay fringes obtained after the spatial interference of the atoms in the condensate. As per the Josephson approximation which we have inculcated, metrological measurements can be performed for a certain time scale after the beginning of the evolution. The Josephson approximation is valid only in this time scale. Beyond this, the two modes  $|1\rangle$  and  $|2\rangle$  change significantly during evolution. This is because of the interaction with the surrounding environment which would induce position dependent phase difference into the fringes obtained from the accumulated differential phase shift.

Basically, when the Josephson approximation breaks down, the  $\hat{J}^2$  term in the two mode hamiltonian dominates. As mentioned, this term is responsible for phase diffusion (loss of information) and entanglement with the surroundings. To get the solutions of these dynamics of the two hyper-fine levels, we need to know the solutions of the time-dependent, coupled Gross Pitaevskii equation below

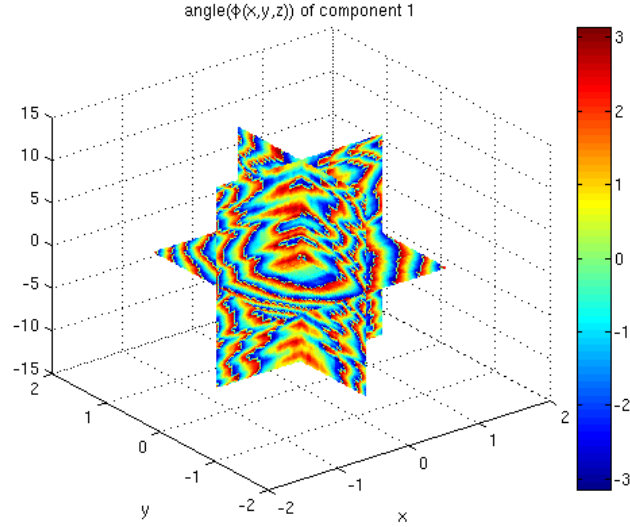


Figure 7.6:  $\psi_{N,1}$

$$i\hbar \frac{\partial \psi_{N,\alpha}}{\partial t} = \left( -\frac{\hbar^2}{2m} \nabla^2 + V + \sum_{\beta=1}^2 g_{\alpha,\beta} N_{\beta} (|\psi_{N,\beta}|^2) \right) \psi_{N,\alpha} \quad (7.22)$$

$\alpha$  being 1 and 2 means the existence of wave function in the two hyper-fine modes.  $N_1$  and  $N_2$  being the number of atoms in both the modes. The quantity  $Im(\langle \psi_{N1} | \psi_{N2} \rangle)$  represents the spatial overlap of the two mode wave functions. In a simpler language, how clear a fringe is obtained is what is being observed.

The wave functions of the two modes before they spatially evolve separately looks as follows. For  $|1\rangle$  hyper-fine level, it is given above

Whereas for the atoms in  $|2\rangle$ , the wave function looks as give below

The detection probabilities for each hyper fine level ( $|1\rangle$  and  $|2\rangle$ ) which is calculated involving the Josephson approximation looks as follows

$$p_{1,2} = \frac{1}{2} [1 \mp Im(\langle \psi_{N1} | \psi_{N2} \rangle)] \quad (7.23)$$

$$\langle \psi_{N1} | \psi_{N2} \rangle = \int d^3r \psi_{N,2}^* \psi_{N,1}$$

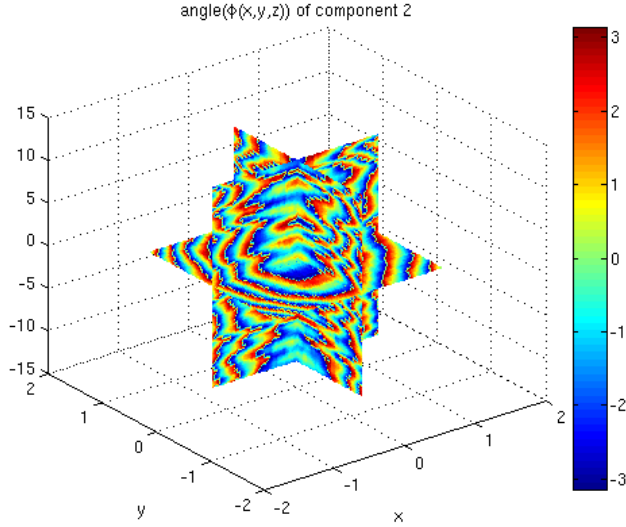


Figure 7.7:  $\psi_{N,2}$

But ideally, the the probabilities would look like

$$p_{1,2} = \frac{1}{2}[1 \mp \sin \Omega_N t] \quad (7.24)$$

where  $\Omega_N$  is the fringe frequency given as

$$\Omega_N = \frac{N\eta_N\gamma_1}{\hbar} \quad (7.25)$$

$\gamma_1$  is the coupling constant which we are going to estimate.

The graph for Ramsay fringes for a 1000 atom rubidium BEC is shown below:

We observe that when the longitudinal potential gets harder, i.e for increasing value of  $q$ , the fringes obtained are much more clearer and close to the idealized fringe frequency. This happens when we observe with respect to increasing time when the modes tend not to retain their wave function.

This behaviour of fringe pattern can be observed for higher number of atoms, say 5000. Here the behaviour digresses from the idealized frequency at the very beginning of the time

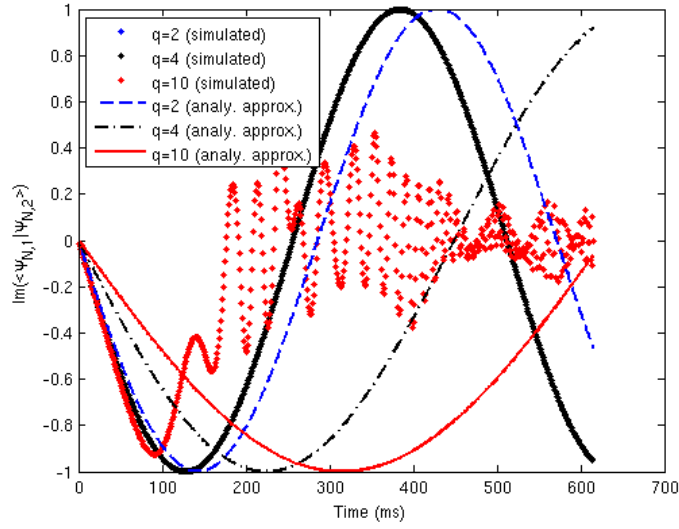


Figure 7.8: Ramsay fringes for  $^{87}\text{Rb}$  BEC for  $N=1000$  atoms

interval. Here too, the visibility of the fringe gets better with the hardness of the trap. Ramsay fringes for a BEC of 5000 atoms is given below

The uncertainty in estimation of the coupling constant of the condensate can be obtained from the Ramsay fringes obtained. According to the error estimation formula, the error is proportional to  $N$  as follows

$$\delta\gamma_1 = \frac{\langle (\Delta \hat{J}_y)^2 \rangle^{1/2}}{\left| d \langle \hat{J}_y \rangle / d\gamma_1 \right|} = \frac{1}{N^{3/2} \eta_N} \quad (7.26)$$

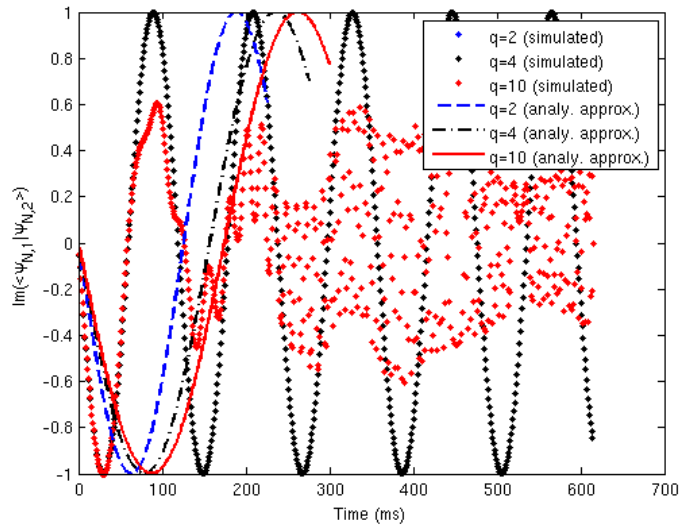


Figure 7.9: Ramsay fringes for  $^{87}\text{Rb}$  BEC for  $N=5000$  atoms



# Chapter 8

## Conclusion

We observe that the sensitivity scaling we have obtained is better than the Heisenberg scaling which scales as  $N^{1/2}$  for nonlinear Ramsay interferometry performed using a two-mode Bose Einstein condensate using rubidium-87 atoms. This increased precision enhances the use of quantum metrology extensively in various fields. Although, the numerical simulations can also be performed when the position-dependent phase shift is acquired for a little longer time scales. It is interesting to analyze the Ramsay fringes obtained for this phase shift before the two modes spatially separate with time.

# Bibliography

- [1] M. A. Nielsen, I. L. Chuang, Quantum Computation and Quantum Information (Cambridge Univ. Press, Cambridge, 2000)
- [2] G. Tóth and I. Apellaniz, J. Phys. A 47, 424006 (2014)
- [3] P. Kok, S. L. Braunstein, J. P. Dowling, J. Opt. B Quantum Semiclass. Opt. 6, 5811 (2004)
- [4] Zwiernz, M., Pérez-Delgado, C. A. and Kok, P. General optimality of the Heisenberg limit for quantum metrology. Phys. Rev. Lett. 105, 180402 (2010)
- [5] Boixo, S., Datta, A., Shaji, A. and Caves, C.M., 2010. Nonlinear interferometry with Bose-Einstein condensates. Physical Review A, 82(5), p.053636. Vancouver
- [6] M. Kitagawa and M. Ueda, Phys. Rev. A 47, 5138 (1993)
- [7] S. Jesenko, M. Znidaric, "Ultracold atoms in optical lattice", Seminar, Univerza v Ljubljani, Fakulteta za matematiko in fiziko (2010)
- [8] Maccone, L., 2013. Quantum metrology: why entanglement?. arXiv preprint arXiv:1304.7609. Vancouver
- [9] V., Lloyd, S. and Maccone, L., 2004. Quantum-enhanced measurements: beating the standard quantum limit. Science, 306(5700), pp.1330-1336.
- [10] Peng, C.Z., Deng, Y., Barbieri, M., Nunn, J. and Walmsley, I.A., 2013. Sequential path entanglement for quantum metrology. Scientific reports, 3, p.1779.
- [11] L., Rossi, M.A. and Paris, M.G., 2017. Quantum metrology beyond the quantum Cramér-Rao theorem. Physical Review A, 95(1), p.012111.
- [12] Wu, S., Zhong, H. and Lee, C., 2014. Quantum metrology with cold atoms. In Annual Review of Cold Atoms and Molecules (pp. 365-415).
- [13] B.J., 2007. Two-mode theory of BEC interferometry. Journal of Modern Optics, 54(5), pp.615-637.

- [14] Datta, A., Davis, M.J., Shaji, A., Tacla, A.B. and Caves, C.M., 2009. Quantum-limited metrology and Bose-Einstein condensates. *Physical Review A*, 80(3), p.032103.
- [15] WRIGHT, T., Gasenzer, T., Gardiner, S.A. and Proukakis, N.P., 2017. Formation of Bose-Einstein condensates. *Universal Themes of Bose-Einstein Condensation*, p.117.
- [16] Vinas, X., 2000. Thomas-Fermi approximation for Bose-Einstein condensates in traps. *Physical Review A*, 61(4), p.043603.